

Numerical Computation of Signal Stimulation from Ligand-EGFR Binding During Invadopodia Formation

Noorehan Yaacob*, Nur Azura Noor Azhuan, Sharidan Shafie and Mohd Ariff Admon

¹Department of Mathematical Sciences, Universiti Teknologi Malaysia
81310 UTM Johor Bahru, Malaysia

*Corresponding author: noorehanyaacob@gmail.com

Article history

Received: 10 November 2019

Received in revised form: 21 November 2019

Accepted: 24 December 2019

Published online: 31 December 2019

Abstract Invadopodia are finger-like protrusions located at subcellular membrane which can lead to cancer cell invasion. The formation of invadopodia involves several steps such as actin polymerizations, degradation of extracellular matrix which produce ligand and signal stimulation that is occurred from the binding of ligand with epidermal growth factor receptor. In this paper, a mathematical model of signal transduction is investigated. Both signal and ligand are represented by Laplace equation with Dirichlet boundary condition for each region. The cell membrane is treated as free boundary surface to separate any activity that occurred in intracellular and extracellular regions. The motion of the interface is taken as gradient of interior signal and the cell membrane is set as zero level set function. The problem is solved numerically using finite difference scheme of upwind, interpolation and extrapolation methods. The results showed that the formation of invadopodia is formed when protrusions exist on the cell membrane.

Keywords Mathematical modeling; cancer cell invasion; invadopodia formation; level set method; free boundary interface.

Mathematics Subject Classification

46N60, 92B99.

1 Introduction

Cancer is the second main cause of death and is estimated to be 9.6 million in 2018. Approximately, 1 in 6 deaths are due to cancer. However, in the next two decades, the rate of death related to cancer is anticipated to rise by 70%. The most common types of cancer among men are lung, prostate, colorectal, stomach and liver, while women are usually affected by breast, colorectal, lung, cervix and thyroid cancer. Hence, from this reported data, we can say that cancer is a serious problem to human health [1].

At normal condition, proto-oncogenes are responsible for cell division and growth but during genetic mutation, they become oncogenes that are dangerous for the existing cell. The

stimulation of the uncontrolled cell division is due to deficiency of tumor suppressor genes. Therefore, in the past three decades, studies on substantial volume of information about genes and proteins with their relationship to cancer growth have been conducted [2–4]. Recently, the role of mutated genes in cancer cells has become very important. Hence, the potency of gene expression and defective proteins is considered in [5] to detect the novel cancer biomarkers.

The study of biophysical model of tumor invasion has been conducted in [6]. This model consist of three coupled partial differential equations (PDEs) to describe the interaction of cancer cell density, extracellular matrix (ECM) density and matrix degrading enzyme concentrations. The relation between cancer cells and the host tissue is considered in this model in order to investigate the effect of tumor growth and invasion in the real biological phenomena. At the same time, [6] has proposed a computational model to predict the location and shape of tumor in realistic geometries at particular instance. The PDEs are discretized in space using Galerkin finite elements and in time using Crank-Nicolson method [7].

The occurrence of cancer cells is the consequence of malignant transformation [8]. The genetic instability of genetic causes the cell to proliferate and form a tumor. These biological capabilities are known as the features of cancer which include self-sufficiency in proliferative signaling, evasion of growth suppressors, apoptosis, secretion of pro-angiogenic signals, invasion and metastasis. Metastasis is defined as the migration of the tumor cell from the normal location to invade another tissue or organ. Metastatic cancer cells have to penetrate several physical barriers to escape from the primary tumor before spreading to the other tissue or organ. In order to pass through these barriers, the F-actin rich protrusions or invadopodia are formed. Hence, these invadopodia will degrade the ECM and enable the invasive tumor cells pass through it [9, 10].

Invadopodia are obtained from the stimulation of signal that make a branched actin assembly at the sites of membrane [11]. The main factor that contributes to this process is the degradation of ECM mediated by subcellular actin-rich structures. For the process of ECM degradation, membrane type 1 metalloprotease (MT1-MMP) is the most important proteinase in invadopodia. However, in addition to MT1-MMP proteinase that encouraged to ECM degradation, many other proteinases that work together are secreted at invadopodia. Hence, [12] has listed the proteins related to the formation of invadopodia which are responsible for high levels of proteolysis throughout cancer invasion and metastasis. Thus, these can be considered as crucial in cancer invasion.

The study on invadopodia has attracted the attention of many researchers for many years. In the effort to understand more about the formation and maturation of invadopodia, [13] has proposed a positive feedback loop. The positive feedback loop is rendered from the view of biology, which includes the integration of several processes that consist of reorganization of actin, degradation of ECM, the process of signal through epidermal growth factor receptor (EGFR) and matrix metalloprotease (MMP) synthesis and delivery to the location of the invading front. In this study, the rate constant of MMP is varied. Hence, it is found that the cancer cells become more invasive as the rate constant of MMP is larger.

The velocity of membrane is considered as the gradient of inner signal that initiates the movement of interface. Related to this situations, [14] has studied a free boundary problem for the formation of protrusions. To deal with the velocity of membrane, level set method is used so that discontinuities near the interface are avoided. The models consist of Laplace equation with Dirichlet condition inside the cell while using Neumann condition on the outside. In solving

this model, first order Cartesian finite difference method is employed. The level set methods are algorithms for tracing the boundaries and interfaces in the progression of time [15, 16].

In [17], the problem on the signal transduction in invadopodia formation is solved by using a fixed domain method. In this method, free boundary is converted to fixed boundary domain. Signal transduction through the binding between ligand and membrane associated receptor is important in order to establish the actin polymerization and then push the membrane of migrating cells. In [17], one-dimensional Stefan-like problem of signal transduction and cell membrane is treated as free boundary surface to separate any activity that occurred in intra- and extracellular region. The movement of the free boundary or velocity is calculated by the decrease of signal gradient on the front. The numerical results indicate that both free boundary positions and signal distributions are increased as time progresses.

Mathematical modeling is one of the methods to understand the mechanism of cancer, which includes the cancer growth, cancer invasion and many more. In addition, mathematical approaches using continuous and discrete models, particularly by considering partial and ordinary differential equations in tumor growth, play a role in the relationship between mathematics and oncology which is a branch of medicine [18]. Several mathematical models and approaches have made it possible to obtain some insights into the dynamics of cancer invasion. Hence, it is one of the effective methods to access the intricate processes such as infection dynamics and one of the best tools to test hypotheses on the ideal way to control the spread of an infection [19]. On the other hand, the development, invasion and metastasis of breast cancer incorporated with the biological phenomena can be generated using mathematical models [20].

From the fact that signal plays an important role during the formation of invadopodia, the extension study from [14, 18] are done. In this study, the formation of invadopodia is investigated in contributions to several steps such as degradation of ECM which produce ligand, signal transduction that is stimulated from the binding of ligand and EGFR and the movement of the interface with normal velocity.

2 The Model

2.1 Mathematical Modeling

In this section, three variables including the ligand density, $c^*(\mathbf{x}, t)$, the signal density, $\sigma(\mathbf{x}, t)$ and the velocity on the plasma membrane, $v(\mathbf{x}, t)$ are investigated. The interaction between the variables in this study is defined in the domain $\Omega = O_t^* \cup \Gamma_t \cup O_t^\sigma$ as shown in Figure 1. It is defined by $\Omega = O_t^\sigma \cup \Gamma_t \cup O_t^{c^*}$. MMPs degrade the ECM. From this degradation, ligand is created. Ligand binds to the receptor on the plasma membrane and stimulates signaling pathway which causes up-regulation of MMPs. Assume that at any time t , the cell membrane carries the flux of membrane-type 1 matrix metalloproteinase (MT1-MMP) defined as a function, $g(\mathbf{x})$ where $g(\mathbf{x}) = 0.1[2 + \cos(3\pi(x + y)) \cos(\pi(x + 0.3))]$, [14]. The matrix metalloproteinases (MMPs) play an important role in degrading the extracellular matrix (ECM) and hence produce the ligand on the cell boundary.

The ligand binds to the receptor on the plasma membrane and hence stimulates signal inside the cell. The membrane is moved with normal velocity on the interface and the velocity is interpreted as the gradient of the inner signal, [14, 18]. In the real biological phenomena, the formation of invadopodia consists of several processes including the production of MMP

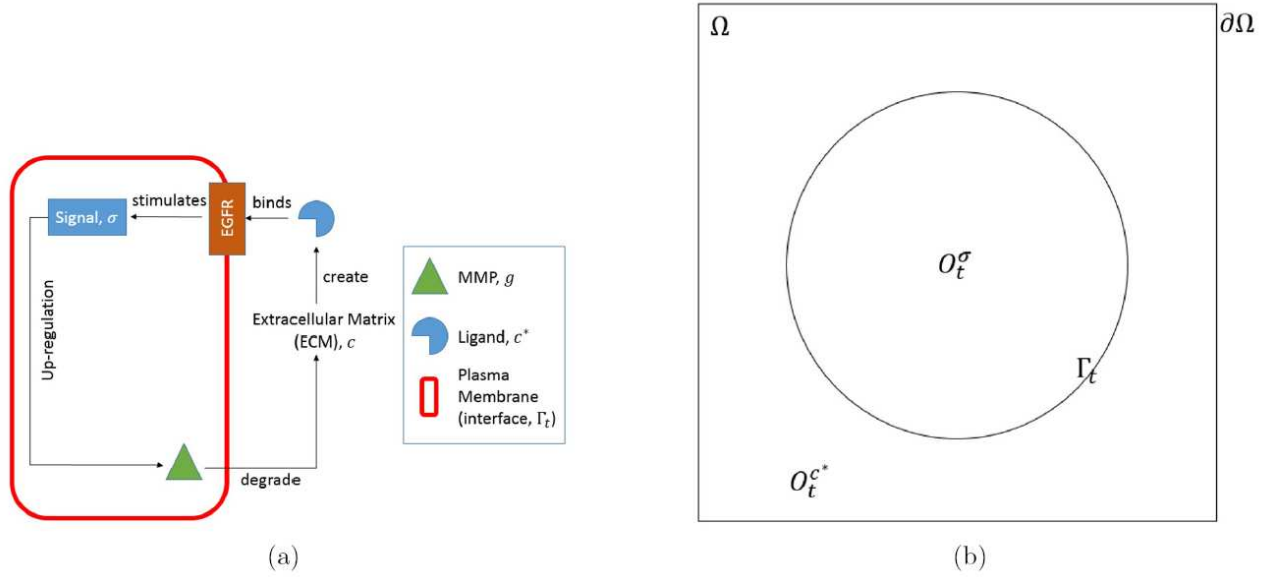


Figure 1: The schematic diagram of (a) the molecular interactions involved for invadopodia formation and (b) the geometrical setting of the complete domain for two dimensional invadopodia formation.

enzymes, actin polymerizations and others, but in this study, these processes are excluded. Note that, we only consider steady case problem in which the time derivative is not considered for both ligand and signal density. For protrusions formation, [14] agreed that the dynamics are much faster than the characteristics of time.

Therefore, this study explored the cancer cell problem associated with the formation of invadopodia in two-dimensional signaling pathways. The mathematical modeling on the invadopodia formation is governed by the following system of differential equations

1. For ligand:

$$\begin{aligned} \Delta c^* &= 0, & \mathbf{x} \in O_t^{c^*}, & \quad \mathbf{x} \in (x, y), \\ c^*|_{\partial\Omega} &= 0, \\ c^*|_{\Gamma_t} &= g|_{\Gamma_t}, & t \in [0, T]. \end{aligned} \tag{1}$$

2. For signal:

$$\begin{aligned} \Delta \sigma &= 0, & \mathbf{x} \in O_t^\sigma, & \quad \mathbf{x} \in (x, y), \\ \sigma|_{\Gamma_t} &= g|_{\Gamma_t}, & t \in [0, T]. \end{aligned} \tag{2}$$

3. For velocity:

$$\mathbf{v} = \nabla \sigma, \quad \mathbf{v} \in (x, y). \tag{3}$$

The cell membrane is taken by the zero level set function, $\psi(\mathbf{x}, t)$ which satisfies the equation of transport $\partial_t \psi + \mathbf{v} \cdot \nabla \psi = 0$, where the velocity is extended from $\nabla \sigma|_{\Gamma_t}$. Extension of velocity is significant so that the discontinuities across the interface with the whole domain can be avoided. Specifically, the velocity extension, \mathbf{w} in the whole domain is evaluated using:

4. For velocity extension:

$$\begin{aligned} (\nabla\psi \cdot \nabla)\mathbf{w} &= 0, & \text{in } \Omega, & \mathbf{w} \in (x, y), \\ \mathbf{w} &= \mathbf{v} & \text{on } \Gamma_t. \end{aligned} \tag{4}$$

2.2 Non-dimensionalization

The equation system are dimensionalized in order to use realistic parameter values. The parameters of c_0^* , σ_0 , v_0 and w_0 are densities at the chemical equilibrium [13]. Hence, setting

$$\tilde{c}^* = \frac{c^*}{c_0^*}, \quad \tilde{\sigma} = \frac{\sigma}{\sigma_0}, \quad \tilde{\mathbf{v}} = \frac{\mathbf{v}}{v_0}, \quad \tilde{\mathbf{w}} = \frac{\mathbf{w}}{w_0},$$

we have our non-dimensionalized model by dropping tildes

1. For ligand:

$$\begin{aligned} \Delta c^* &= 0, & \mathbf{x} \in O_t^c, & \mathbf{x} \in (x, y), \\ c^*|_{\partial\Omega} &= 0, \\ c^*|_{\Gamma_t} &= g|_{\Gamma_t}, & t \in [0, T]. \end{aligned} \tag{5}$$

2. For signal:

$$\begin{aligned} \Delta \sigma &= 0, & \mathbf{x} \in O_t^\sigma, & \mathbf{x} \in (x, y), \\ \sigma|_{\Gamma_t} &= g|_{\Gamma_t}, & t \in [0, T]. \end{aligned} \tag{6}$$

3. For velocity:

$$\mathbf{v} = \nabla \sigma, \quad \mathbf{v} \in (x, y). \tag{7}$$

4. For velocity extension:

$$\begin{aligned} (\nabla\psi \cdot \nabla)\mathbf{w} &= 0, & \text{in } \Omega, & \mathbf{w} \in (x, y), \\ \mathbf{w} &= \mathbf{v} & \text{on } \Gamma_t. \end{aligned} \tag{8}$$

2.3 Numerical Computation

Equations (5) to (8) are solved using finite difference scheme of upwind, ghost fluid method with linear extrapolation and level set method. The difficulties in this study are to deal with regular and neighboring points on the interface (plasma membrane). By using the finite difference method, first, we should take note of the grid points that lies at regular or neighboring points. Regular points are defined as the points that are located far from the interface while neighboring points are the points that are very close to the interface. In order to avoid the discontinuities across the interface, two numerical values are identified on the grid points, including the points that are exactly on the grid and ghost values of the points that are extrapolated from the other side of the interface [21]. Therefore, the numerical algorithm that is used in this study is as follows:

1. For the regular point I , second order of x -derivative with centered difference is

$$\nabla u_{i,j}^0 = \frac{u_{i+1,j}^0 - 2u_{i,j}^0 + u_{i-1,j}^0}{h^2}, \tag{9}$$

where the variable u denotes the ligand or signal density.

2. For the neighboring point N , second order of x -derivative with centered stencil of ghost fluid method is

$$\nabla u_{i,j}^0 = \frac{2}{(1 + \theta_x)h^2} u_{i+1,j}^0 - \frac{2}{\theta_x h^2} u_{i,j}^0 + \frac{2}{\theta_x(1 + \theta_x)h^2} u_{i+\theta_x,j}^0. \quad (10)$$

3. The plasma membrane is taken as zero level set function such that $\Gamma_t = \{\mathbf{x} \in \Omega, \psi(\mathbf{x}, t) = 0\}$ and the initial interface, $\psi(\mathbf{x}, t)$ is considered as

$$\psi_{i,j}^0 = x_i^2 + y_j^2 - r^2, \quad (11)$$

where r is the radius of a cell (assumed circle shaped).

4. The θ_x in (6) is defined as the distance of the point x_i to the interface, Γ_t and is calculated using

$$(\theta_x)_{i,j}^0 = \begin{cases} \frac{\psi_{i,j}^0}{\psi_{i,j}^0 - \psi_{i-1,j}^0}, & \mathbf{x} \in [x_{i-1,j}, x_{i,j}], \\ -\frac{\psi_{i,j}^0}{\psi_{i+1,j}^0 - \psi_{i,j}^0}, & \mathbf{x} \in [x_{i,j}, x_{i+1,j}]. \end{cases} \quad (12)$$

5. The velocity, \mathbf{v} in the signal x -region is computed using

$$(v_x)_{i,j}^0 = \begin{cases} \frac{\sigma_{i+1,j}^0 - \sigma_{i-1,j}^0}{2h}, & \text{for } I, \\ \frac{\sigma_{i,j}^0 - \sigma_{i-1,j}^0}{h}, & \text{for } N^+, \\ \frac{\sigma_{i+1,j}^0 - \sigma_{i,j}^0}{h}, & \text{for } N^-, \end{cases} \quad (13)$$

where N^- and N^+ are the set of neighboring points on the left and right sides respectively.

6. The velocity inside the interface is extended to the exterior cell region using formula of $(\nabla\psi \cdot \nabla)\mathbf{w} = 0$, therefore

$$(\psi_x)_{i,j}^0 = \begin{cases} \frac{\psi_{i,j}^0 - \psi_{i-1,j}^0}{h}, & \text{for } \partial\Omega^+, \\ \frac{\psi_{i+1,j}^0 - \psi_{i,j}^0}{h}, & \text{for } \partial\Omega^-, \\ \frac{\psi_{i+1,j}^0 - \psi_{i-1,j}^0}{2h}, & \text{otherwise.} \end{cases} \quad (14)$$

$$(w_x)_{i,j}^0 = \begin{cases} \frac{w_{i,j}^0 - w_{i-1,j}^0}{h}, & \text{if } \psi_x > 0, \\ \frac{w_{i+1,j}^0 - w_{i,j}^0}{h}, & \text{if } \psi_x < 0, \end{cases} \quad (15)$$

where $\partial\Omega^-$ and $\partial\Omega^+$ are the left and right boundaries respectively. Notice that, on the interface, $\Gamma_t, \mathbf{v} = \mathbf{w}$.

7. The level set function, $\psi(\mathbf{x}, t)$ is updated using

$$\psi_{i,j}^1 = \psi_{i,j}^0 - \Delta t [((v_x)_{i,j}^0)((\psi_x)_{i,j}^0) + ((v_y)_{i,j}^0)((\psi_y)_{i,j}^0)], \quad (16)$$

where $(\psi_x)_{i,j}^0$ and $(\psi_y)_{i,j}^0$ is using second order upwind technique.

3 Results and Discussion

New modeling is introduced in [18] in order to overcome the problem observed in [13]. The new variable of signal transduction is emphasized. Also, the plasma membrane is treated as a free boundary interface. In his study, the other variables is excluded for simplicity. Hence, in this paper, the ligand density is considered since signal is stimulated from the binding of ligand with epidermal growth factor receptor (EGFR). Study in [18] focused on one-dimensional problem, however, in this study, two-dimensional is conducted to get clear view of the invadopodia formation.

Ligand and signal stimulation are computed using finite difference scheme of upwind, ghost fluid method with linear extrapolation and also level set method. In this study, the domain, Ω is measured in a square with dimension $[-L, L] \times [-L, L]$ where L is taken as 1. In (11), the radius of the circle is set as $r = 0.6667$. From the results obtained, the appearance of invadopodia is discussed.

Figure 2 showed the initial interface of cancer cell where the blue line of the circle indicates the plasma membrane of the cell. After a time step, the formation of invadopodia can be seen where the protrusions are generated at the membrane as in Figure 3. This result indicates that the invadopodia are formed with the presence of signal that is stimulated from ligand and epidermal growth factor receptor binding.

Based on Figures 4 and 5, the maximum density of ligand and signal can be seen at the interface. The yellow colors located near to the interface indicate the high density of ligand and signal. Here, the protrusions are formed as in Figure 3. Since this study is only focused on the steady case, the ligand and signal distributions for initial and after a timestep are similar.

4 Conclusion

This study was aimed at modeling of invadopodia formation that are observed by the presence of finger-like protrusions. The model consists of the system of Laplace operator for ligand and signal densities, in addition to the gradient of signal. The signal is important for the formation of invadopodia. Hence, the role of ligand is the most crucial since the signal is stimulated from the binding of ligand and epidermal growth factor receptor. The movement of the membrane is a consequence of the gradient of signal inside the cell. Meanwhile, the membrane is treated as a free boundary and is considered as zero level set function initially.

The ligand, signal and velocity variables are solved numerically using finite difference scheme of upwind, linear extrapolation, ghost fluid method and level set method. After a timestep, the protrusions are spotted on the interface. Last but not least, several protrusions are formed at the location of high density of ligand and signal. Hence, from this result we can observe that, the high density of ligand and signal can lead to the formation of protrusions on the interface. In conclusion, the protrusions or invadopodia are developed on the membrane due to the presence of signal density inside the cell.

Acknowledgment

The author would like to thank to the Kementerian Pendidikan Tinggi(KPT), Malaysia for the scholarship under MybrainSC scheme and UTM Research Management Centre through FRGS grant (5F098) for the research funding.

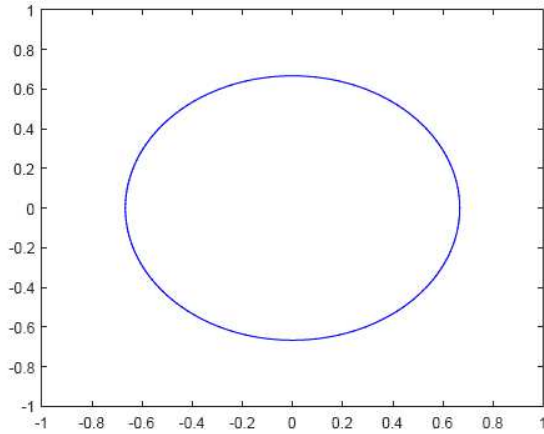


Figure 2: The initial interface for psi.

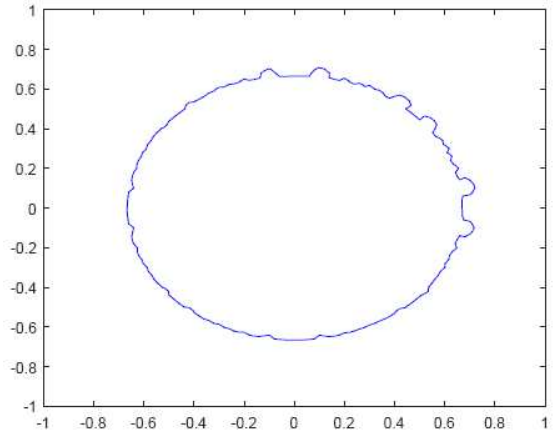


Figure 3: The interface for psi after a time step.

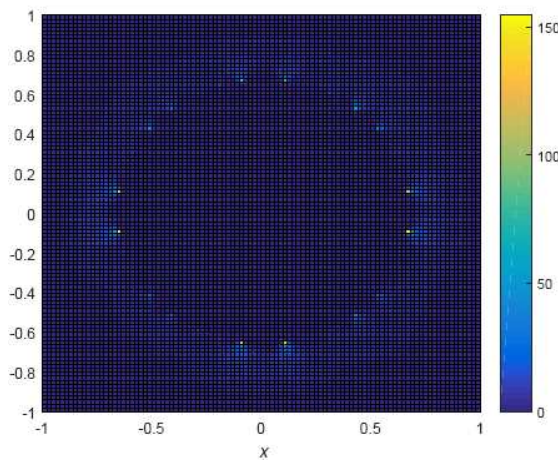


Figure 4: The ligand distribution.

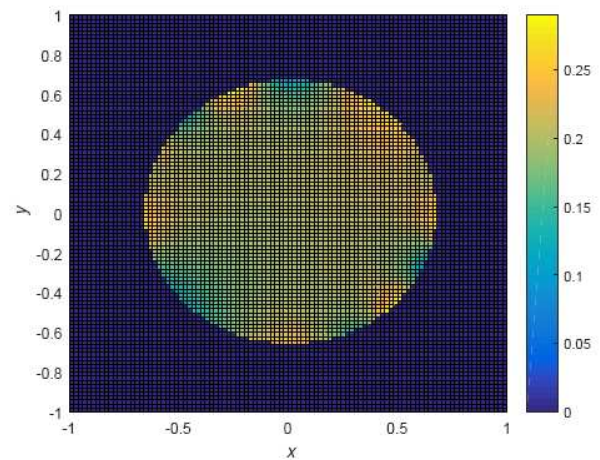


Figure 5: The signal distribution.

References

- [1] Organisation, W. H. Cancer. 2018. URL <https://www.who.int/cancer/en/>. accessed = 2018-12-08.
- [2] Shufen, L., Jingming, L., Chen, C., Rongsheng, Z. and Kankan, W. Pan-cancer analysis of long non-coding rna neat1 in various cancers. *Genes & diseases*. 2018. 5(1): 27–35.
- [3] Francesca, Z., Michelangelo, C. and Stefano, P. Yap/taz at the roots of cancer. *Cancer cell*. 2016. 29(6): 783–803.
- [4] Gerard, B. L., Daria, V. G. and Scott, A. A. Exploiting the epigenome to control cancer-promoting gene-expression programs. *Cancer cell*. 2016. 29(4): 464–476.
- [5] Hassanpour, S. H. and Dehghani, M. Review of cancer from perspective of molecular. *Journal of Cancer Research and Practice*. 2017. 4(4): 127 – 129. ISSN 2311-3006. doi: <https://doi.org/10.1016/j.jcrpr.2017.07.001>.

- [6] Ganesan, S. and Lingeshwaran, S. A biophysical model of tumor invasion. *Communications in Nonlinear Science and Numerical Simulation*. 2017. 46: 135 – 152. ISSN 1007-5704. doi: <https://doi.org/10.1016/j.cnsns.2016.10.013>.
- [7] Ganesan, S. and Lingeshwaran, S. Galerkin finite element method for cancer invasion mathematical model. *Computers & Mathematics with Applications*. 2017. 73(12): 2603 – 2617. ISSN 0898-1221. doi:<https://doi.org/10.1016/j.camwa.2017.04.006>.
- [8] Szabó, A. and Merks, R. M. H. Cellular potts modeling of tumor growth, tumor invasion, and tumor evolution. In *Front. Oncol.* 2013.
- [9] Sibony-Benyamini, H. and Gil-Henn, H. Invadopodia: the leading force. *European journal of cell biology*. 2012. 91 11-12: 896–901.
- [10] Meirson, T. and Gil-Henn, H. Targeting invadopodia for blocking breast cancer metastasis. *Drug Resistance Updates*. 2018. 39: 1 – 17. ISSN 1368-7646. doi: <https://doi.org/10.1016/j.drug.2018.05.002>.
- [11] Parekh, A. and Weaver, A. M. Regulation of invadopodia by mechanical signaling. *Experimental Cell Research*. 2016. 343(1): 89 – 95. ISSN 0014-4827. doi: <https://doi.org/10.1016/j.yexcr.2015.10.038>.
- [12] Hastie, E. L. and Sherwood, D. R. A new front in cell invasion: The invadopodial membrane. *European Journal of Cell Biology*. 2016. 95(11): 441 – 448. ISSN 0171-9335. doi:<https://doi.org/10.1016/j.ejcb.2016.06.006>. Integrated mechano-chemical signals in invasion.
- [13] Saitou, T., Rouzaimaimaiti, M., Koshikawa, N., Seiki, M., Ichikawa, K. and Suzuki, T. Mathematical modeling of invadopodia formation. *Journal of Theoretical Biology*. 2012. 298: 138 – 146. ISSN 0022-5193. doi:<https://doi.org/10.1016/j.jtbi.2011.12.018>.
- [14] Gallinato, O., Ohta, M., Poignard, C. and Suzuki, T. Free boundary problem for cell protrusion formations: theoretical and numerical aspects. *Journal of Mathematical Biology*. 2017. 75(2): 263–307. ISSN 1432-1416. doi:10.1007/s00285-016-1080-7.
- [15] Strychalski, W., Adalsteinsson, D. and Elston, T. Simulating biochemical signaling networks in complex moving geometries. *SIAM Journal on Scientific Computing*. 2010. 32(5): 3039–3070. doi:10.1137/090779693.
- [16] Shaikh, J., Bhardwaj, R. and Sharma, A. A ghost fluid method based sharp interface level set method for evaporating droplet. *Procedia IUTAM*. 2015. 15: 124 – 131. ISSN 2210-9838. doi:<https://doi.org/10.1016/j.piutam.2015.04.018>. IUTAM Symposium on Multi-phase Flows with Phase Change: Challenges and Opportunities.
- [17] Admon, M. A. and Suzuki, T. Signal transduction in the invadopodia formation using fixed domain method. *Journal of Physics: Conference Series*. 2017. 890: 012036. doi: 10.1088/1742-6596/890/1/012036.
- [18] Admon, M. A. *Mathematical Modeling and Simulation in an Individual Cancer Cell Associated with Invadopodia Formation*. Osaka University, Japan: Ph.D. Thesis. 2015.
- [19] Braud, G. Mathematical models and vaccination strategies. *Vaccine*. 2017. 36. doi: 10.1016/j.vaccine.2017.10.014.

- [20] Simmons, A., Burrage, P., Nicolau, D. V., Lakhani, S. and Burrage, K. Environmental factors in breast cancer invasion: a mathematical modelling review. *Pathology*. 2017. 49. doi:10.1016/j.pathol.2016.11.004.
- [21] Coco, A. and Russo, G. Second order finite-difference ghost-point multigrid methods for elliptic problems with discontinuous coefficients on an arbitrary interface. *Journal of Computational Physics*. 2018. 361: 299 – 330. ISSN 0021-9991. doi: <https://doi.org/10.1016/j.jcp.2018.01.016>.